Article

New Advances in the Modeling and Verification of Experimental Information for Ester−Alkane Solutions: Application to a Batch-Distillation Case

Juan Ortega,* Luis Fernández, Adriel Sosa, Beatriz Lorenzo, Raúl Ríos, and Jaime Wisniak

Cite This: *Ind. Eng. Chem. Res.* 2020, 59, 8346−8360

Read Online

ACCESS | Metrics & More | Article Recommendations | SI Supporting Information

ABSTRACT: This work shows a practical experience involving the following sequence of tasks on eight binary solutions of alkyl (propyl, butyl) propanoate with four alkanes (hexane to nonane): experimentation → modeling ↔ verification → simulation. Thermodynamic properties related to dilution processes are determined, in addition to vapor−liquid equilibria at 101.32 kPa (iso-*p* VLE), providing a vast database. Some improvements are proposed for the aforementioned tasks: (a) density values at high temperature and pressure for the pure compounds and their modeling to improve the calculation of activity coefficients, (b) the procedure of multiproperty modeling using an ϵ-constraint multiobjective procedure combined with a genetic algorithm for mixed integer nonlinear problem (MINLP) problems, obtaining a {data + model} set, which is subjected to the third task of thermodynamic validation, and (c) with the methodology established in Wisniak, J. et al. A Fresh Look at the Thermodynamic Consistency of Vapour-Liquid Equilibria Data. *J. Chem. Thermodyn.* **2017**, *105*, 385 395, the consistency of iso-*p* VLE data was confirmed, and the process was assisted by a modification of our own method to guarantee the {model-checking} binomial, increasing the reliability of the experimental data provided and the model obtained. The systems propyl propanoate−octane and butyl propanoate−nonane are azeotropic with coordinates, respectively, at (x_{az} = 0.650; T_{az}/K = 392.4) and (x_{az} = 0.633; T_{az}/K = 417.1). The model obtained for the first system is used to simulate the separation process of that binary with a commercial simulator. After implementing the model, comparison of the results generated by the software produced values close to real ones obtained in a batch distillation in the laboratory, improving the values estimated by the simulator software.
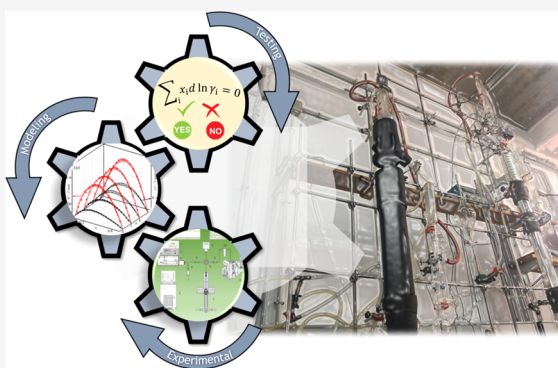
1. INTRODUCTION

Our research group has generated a substantial database totaling more than 35 000 values of properties of binary and ternary solutions, with alkyl esters constituting the basis of a research project. For experimentation (E), important progress has been made in measuring techniques (some still unpublished) in an attempt to improve data quality and to more precisely define the behavior of fluid matter. The mathematical representation or modeling (M) of the experimental data has also been an important area of study, a step closely linked to the previous one, since the quality of the data influences the parameterization of the model. More recently, but along the same line, we have proposed a practical methodology to assess the quality of phase equilibrium data and particularly of vapor−liquid equilibrium (VLE) data. An innovative aspect of this method is the use of a multiproperty approach in which a link between modeling (M) ↔ testing (T) tasks is established, generating a rigorous mathematical−thermodynamic tool of proven efficacy for implementation in simulation (S) calculations and design in chemical engineering.

This work involves a practical application of actions established as EMTS, for a set of eight ester−alkane binary systems, $H_5C_2COOC_vH_{2v+1}$ (v = 3,4) + C_nH_{2n+2} (n = 6−9), extending the database generated and confirming the behavioral structural model for these solutions. Before presenting/accepting these, it will be checked that the information obtained, rigorously modeled by the {data + model} binomial, is reliable for use in development separation operations.

To avoid unnecessary details about the background of these systems, previous information[1−7] and that collected for the purpose of this work is included in Table S1 (Supporting Information, SI). The diagram in Figure 1 shows the previously
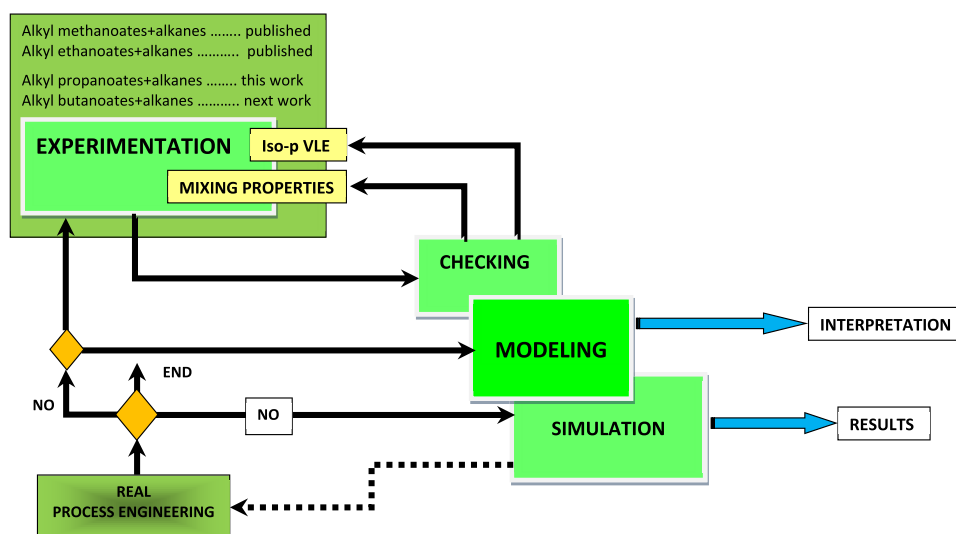
Figure 1. Sequence of tasks for the treatment of the information with properties of solutions and their impact on process engineering.
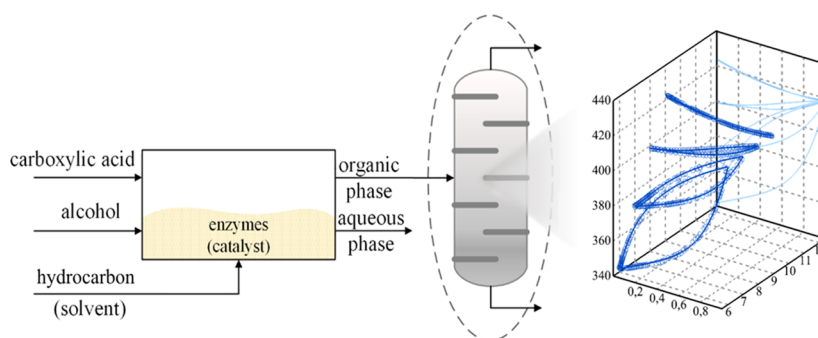

Figure 2. Diagram showing the relevance of distillation in the global esterification process.

mentioned sequence of operations, which will be developed and applied here.

The choice of these systems is justified by (a) providing new experimental information to the database started years ago to rigorously define the behavior of the widest diversity of binary solutions of polar/nonpolar compounds, for which new advances in the {data + model} binomial are proposed and (b) the current interest in improving the efficacy of enzymatic esterification, one of the most promising green alternatives to traditional acid-catalyzed processes, which will be affected by the information contained in the database mentioned in the item (a). The diagram in Figure 2 justifies the distillation operation as a purification process of the ester−alkane solutions derived from esterification.

In addition to items (a) and (b), as already mentioned, the extensive database generated allowed the incorporation of certain improvements in the instrumentation used,[8,9] in modeling,[10,11] and in the analysis of data quality.[12,13] In this work, new contributions are presented, improving and expanding the number of experimental data, with density values at high temperatures and pressures, for esters and alkanes. Certain aspects associated with the modeling are modified to extend their application to quantities representing the volumetric effects of solutions so as to increase the capacity of the representation of the model; the definition of the model is improved by applying criteria based on the information theory, as previously proposed.[14] Improvements in experimentation and modeling tasks would not be relevant if the

available data were insufficient; hence, as shown in the diagram in Figure 1, an important verification task is introduced in the method proposed by the authors[13,15] to improve its applicability in the verification of equilibrium data and that of other properties, combining thermodynamic and mathematical formalisms to produce a powerful support tool.

2. EXPERIMENTAL SECTION

2.1. Materials. The compounds used to prepare the solutions were from Aldrich, with commercial purity ≥99%. Before being used, all were degasified with ultrasound for several hours and a 0.3 nm Fluka molecular sieve was added to reduce the moisture. The water content, determined by Karl Fischer, did not exceed 200 ppm in any case, and the final purity, determined by gas chromatography (GC), was slightly better than the initial one given by the manufacturer. Double-distilled water was used to calibrate the equipment, degassing it before use, showing a final conductivity of <1 μS·cm^{-1}. The quality of the compounds was confirmed by determining certain thermophysical properties at atmospheric pressure, two of them, density ρ and refractive index n_D, at T = 298.15 K; see Table S2. In accordance with the study objectives, the densities of the compounds were also determined at several temperatures in the interval [288−328] K and the iso-p expansion coefficients α, with the average values shown in the aforementioned table, which also records the normal boiling point $T_{b,i}^o$·K^{-1}. On the whole, our results are similar to those

reported in the literature,[16−22] validating the quality of the substances used.

2.2. Apparatus and Measurement Procedures.
2.2.1. Properties of Pure Compounds. The purity of the products was verified by a gas chromatograph, Varian GC-450, equipped with an HP-5 column and FID. The moisture was determined using a Mettler-Toledo C20 coulometric titrator. The n_D was measured with an Abbe refractometer, Zuzi-320, with an uncertainty of $n_D \pm 0.0002$, previously calibrated with water.[16] Densities at atmospheric pressure were measured with an Anton Paar digital densimeter, DMA 60/602, with a standard uncertainty of $(\rho \pm 0.02)$ kg·m^{-3}. The densimeter was calibrated using water and nonane and at each of the working temperatures as reported previously,[22] from where values were taken at the different temperatures. To control the temperature of both the densimeter and the refractometer, a Polyscience 1166D recirculating water bath was used to provide thermal stability $(T \pm 0.01$ K).

To obtain the values of (p, ρ, T), an Anton Paar DMA-512 densimeter was used (see Figure 3) with an average
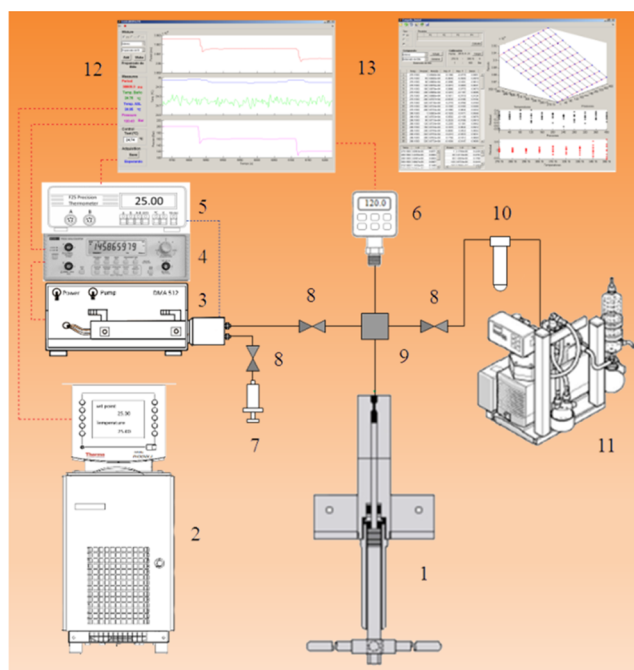
Figure 3. Installation used to measure high-pressure densities. (1) Pressure generator, (2) thermostat bath, (3) densimeter, (4) frequency meter, (5) digital thermometer, (6) digital manometer, (7) syringe, (8) valves, (9) distribution tee, (10) vacuum trap, (11) vacuum pump, (12) data acquisition, and (13) data treatment.

uncertainty in density calculations of $(\rho \pm 0.1)$ kg·m^{-3}. An auxiliary installation was autobuilt in our laboratory, from a similar design to that presented by other authors,[23,24] consisting of a TTi-TF930 frequency counter (4) with a resolution of 0.01%, a recirculating bath, Polyscience 9510 (2) with silicon oil to operate within the interval $T \in [278.15-418.15]$ K; the thermal stability of the cell was $(T \pm 0.01)$ K. The vacuum pump (11), with a capacity of 7 mPa, was used both to clean the installation and to calibrate the densimetric cell, which, together with water, could be used to determine the constants of the apparatus using the data and the procedure proposed by Lagourette et al.[24] The temperature of the sample was measured with a Pt-100 probe connected to

an ASL F25 digital thermometer (5) with a standard uncertainty of the measurement of $(T \pm 0.005)$ K. The HiP system, model 50-6-15 (1), generates different working pressures, which are read on the DMM Evolution digital pressure gauge AE (6), with a reading error of $(0.15\%)p$. The measuring procedure described by other authors[24] was followed.

The instrumentation required to obtain the (T, p_i^o) coordinates and the variables that characterize the iso-p VLE (p, T_i, x_i, y_i), such as the ebulliometer[8] and the auxiliary elements, have been described in previous publications.[9,25] The experimental procedure to determine the vapor pressures of the two esters works quasiautomatically, stepwise with increments of 2.5 kPa in the interval $p \in [37-101.32)$ kPa and of 5 kPa when $p \in (101.32-280]$ kPa, at intervals of preset time. These variations are commanded by a PC that controls the dry nitrogen flow and vacuum with an automatic controller, PPC2 Desgranges & Huot, obtaining with fine-tuning a mean oscillation in the pressurization of $(p \pm 0.02)$ kPa at the equilibrium state. The temperature reached at each pressure completes the saturation curve coordinates.

2.2.2. Properties of Solutions. The energies generated in the mixing processes, h^E, of the eight ester + alkane binaries, $H_5C_2COOC_\nu H_{2\nu+1}$ $(\nu = 3,4) + C_n H_{2n+2}$ $(n = 6-9)$, were measured directly in a Calvet conduction calorimeter, MS80D from Setaram, working in quasi-isothermal conditions of $T = 298.15$ and 318.15 K, with control of approximately ± 1 mK. With the electrical calibration and that generated by a known mixing process,[26] h^E values were obtained with a mean reading error lower than $(1\%)h^E$. The measurement procedure has been described in detail in previous studies.[25]

The (T, x_1, ρ) values, obtained with the DMA 60/602 digital densimeter, were employed to measure the mixing volumes and to calculate the v^E of each of the eight binaries, synthetically prepared by weighing within the range of compositions $x \in (0,1)$, with an uncertainty of $x \pm 3 \times 10^{-4}$. The data set (T, x_1, ρ, v^E) for the solutions was determined every 10 K, between 288.15 and 328.15 K, calibrating the apparatus as indicated. The mean uncertainty of the v^E was $(v^E \pm 2 \times 10^{-9})$ m^3·mol^{-1}.

The procedure used to obtain the iso-p VLE data was previously described.[9] After reaching equilibrium, with quasiconstant values of p and T, the compositions of the liquid, x_i, and vapor phases, y_i, were determined by densimetry. The density of the samples in each phase, ρ, is introduced into eq 1. When resolved by linear regression, this gives rise to a value of $w_i = x_i$ or y_i, depending on whether the sample corresponds to the liquid or vapor phase, respectively.

$$\rho - \sum_{i=1}^{2} \rho_i w_i = w_1 w_2 \sum_{i=0}^{2} \theta_i w_1^i \tag{1}$$

where ρ_i are the densities of the pure compound i. The parameters θ_i were obtained previously at a given temperature and at atmospheric pressure, correlating the coordinate values (w_i, ρ) of the synthetic binary solutions with eq 1. The mean uncertainty in the composition calculated for the liquid phase was around $x \pm 0.002$ and $y \pm 0.003$ for the vapor phase.

The rectification assays were carried out in a packed column 1 m high with an interior diameter of 3 cm, equipped with Raschig rings of 3×3 mm^2. The column head has a magnetic regulator to vary the reflux ratio; the details of the complete installation are shown in Figure 4. The column is fed from a
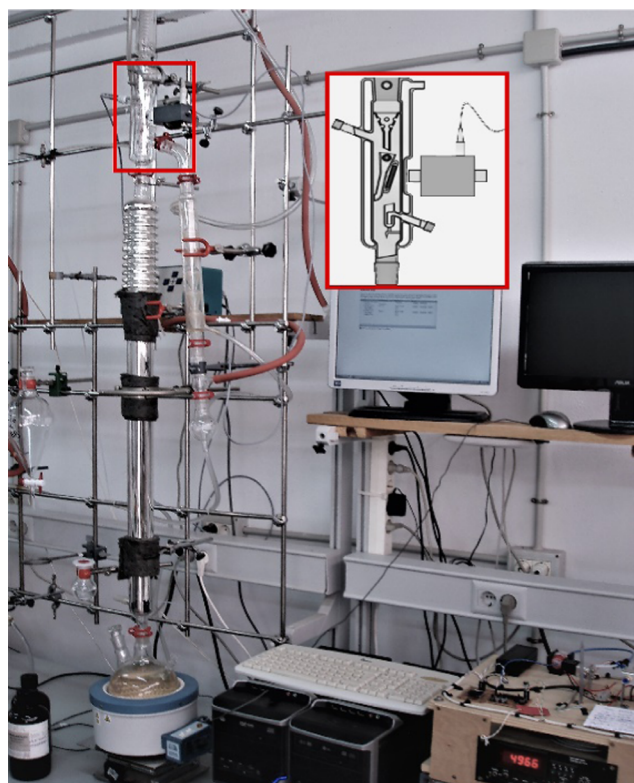
Figure 4. Actual installation of the distillation column and auxiliary elements. The zoomed image shows the reflux system with the magnetic controller.

250 mL flask (reboiler) containing the solution to be separated, where values are recorded for pressure (with a transducer, $p \pm 0.1$ kPa) and temperature (with a Pt-100, $T \pm 0.02$ K). The column head is at atmospheric pressure, $p_a \approx 97.8$ kPa, and the temperature is also recorded using a Pt-100. The condenser is cooled using a Julabo F-25 thermostat bath. In each assay, the column reaches equilibrium with total reflux, and then, it is set to a reflux ratio of 6, which is maintained throughout the experiment, recording the temporal variation of the temperatures at the column head. Samples from the feeding flask and distillate are taken and analyzed by densimetry to study the composition inside the apparatus, which is determined using eq 1 corresponding to the studied solution.

3. PRESENTATION OF RESULTS

3.1. Pure Compounds. *3.1.1. Vapor Pressures.* No vapor pressure values were determined for the four hydrocarbons, taking the data from previous studies.[25,27] The (T, p_i^o) data obtained for the two esters $H_5C_2COOC_\nu H_{2\nu+1}$ ($\nu = 3, 4$) are recorded in Table S3. These coordinates are modeled using the known Antoine's equation using reduced variables.

$$\log_{10} p_i^o /\text{kPa} = A - \frac{B}{T/K - C}$$

$$\text{or } \log_{10} p_{i,r}^o = a - \frac{b}{T_r - c} \quad (2)$$

A nonlinear regression procedure[28] was used for the parameterization, minimizing the following objective function OF

$$\text{OF}(p_i^o) = \left[\sum_{j=1}^{m_p} (p_{i,j,\text{exp}}^o - p_{i,j,\text{cal}}^o)^2 / m_p \right]^{0.5} \quad (3)$$

where m_p corresponds to the number of experimental points in each data series. The parameters obtained for eq 2 are shown in Table 1, where they are compared with values obtained from the literature.[18,19,29,30] Figure S1 shows the deviations of $p_{i,\text{exp}}^o$ relative to those reported by other authors in the temperature range indicated in Table 1 for each compound. The differences observed for propyl propanoate are acceptable, although there is a progressive increase in $e(p_i^o)$ with temperature, with the mean error in this interval being lower than 1%. In contrast, for butyl propanoate, $e(p_i^o)$ tends to decrease with an increase in temperature. The greatest difference with respect to published data[30] could be due to the poorer quality of the previously used ester; however, for this case, the mean error, found to be lower than 4%, had no significant effect on the calculation of activity coefficients. The reduced form of Antoine's equation, eq 2, was used, and the coefficients a, b, and c were determined, giving an estimation of the acentric factor of the compounds, see Table 1, which coincided reasonably well with values reported in the literature and those estimated by the Lee–Kesler method.[31]

3.1.2. p–ρ–T Measurements. What is the purpose of these measurements? One variable that participates in the calculation of activity coefficients γ_i for each compound i in solution is the volume/density at saturation, $v_i^o(T, p) = 1/\rho_i^o(T, p)$, using in previous works[11,25] the modified Rackett equation,[32] one of the most used for this purpose. Although the influence of $v_i^o(T)$ is not very significant on the global computation of γ_i, a rigorous calculus was conducted to find a more suitable model.

Table 1. Coefficients A, B, and C of the Antoine Equation and the Corresponding Standard Deviation $s(p_i^o)$/kPa

compound	A (a)	B (b)	C (c)	$s(p_i^o)$, kPa	ω^a	$T_{\min} - T_{\max}$	refs
propyl propanoate	5.84703 (2.35427)	1166.81 (2.01870)	91.60 (0.1585)	0.05	0.374	365–434	this work
	6.03936	1287.02	76.26		0.373	355–420	29
	6.19565	1383.66	65.07		0.372	330–395	18
					0.374^b		
butyl propanoate	6.23838 (2.79127)	1488.86 (2.50648)	66.71 (0.1123)	0.06	0.474	390–457	this work
	6.27130	1506.00	65.63		0.477	350–422	19
	6.72425	1860.26	23.89		0.469	382–425	30
					0.477^b		

^{a}Values obtained for the Antoine equation and the Pitzer relationship. ^{b}Values estimated by Lee–Kesler.[31] The constants inside the parenthesis (a, b, c) correspond to the parameters of the reduced form of the Antoine equation.

Table 2. Parameters for the Tait−Rackett Combined Equation Obtained in the Modeling of (p, ρ, T) Values

	hexane	heptane	octane	nonane	propyl propanoate	butyl propanoate
$\hat{a}$	6.534×10	6.564×10	6.765×10	5.921×10	4.720×10	3.769
$\hat{b}$	2.749×10^{-1}	2.698×10^{-1}	2.718×10^{-1}	2.525×10^{-1}	2.005×10^{-1}	5.814×10^{-2}
$\hat{c}$	2.739×10^{-1}	3.028×10^{-1}	3.134×10^{-1}	3.438×10^{-1}	3.364×10^{-1}	1.566×10^{-1}
$\hat{d}$	5.075×10^{2}	5.401×10^{2}	5.688×10^{2}	6.471×10^{2}	6.623×10^{2}	6.787×10^{2}
B_0	1.414×10^{3}	-2.964×10^{-1}	-8.042×10^{2}	1.469×10	1.268×10	2.472×10
B_1	2.601×10^{4}	4.763×10^{3}	3.902×10^{3}	2.533×10^{3}	2.210×10^{3}	6.169×10
B_2	-1.609×10	-1.135×10^{-2}	-1.571×10^{-4}	2.985×10^{2}	4.514×10^{2}	1.382×10^{3}
C_0	4.102×10^{-2}	3.807×10^{-2}	5.486×10^{-2}	2.732×10^{-1}	3.723×10^{-1}	1.137
C_1	-3.748×10^{-4}	-2.833×10^{-4}	-3.419×10^{-4}	-1.981×10^{-3}	-2.716×10^{-3}	-7.833×10^{-3}
C_2	1.038×10^{-6}	6.447×10^{-7}	6.442×10^{-7}	4.004×10^{-6}	5.462×10^{-6}	1.475×10^{-5}
ARD	0.141	0.202	0.275	0.041	0.058	0.086
RMSE	1.756	2.308	3.017	0.434	0.639	0.998

Over the recent decades, many researchers have determined the $p-\rho-T$ values of pure compounds at high pressures and temperatures, which, in most cases, tend to be correlated with the well-known Tait equation.[33]

$$\rho_i(p, T) = \rho_{i,0}(T, p_0)\left[1 - C(T)\ln\left(\frac{p + B(T)}{p_0 + B(T)}\right)\right]^{-1}$$

$$p_0/\text{MPa} = 0.1 \tag{4}$$

making

$$\rho_{i,0}(T) = A_0 + A_1 T + A_2 T^2, \quad B(T) = B_0 + B_1 T + B_2 T^2,$$
$$C(T) = C_0 + C_1 T + C_2 T^2 \tag{5}$$

This modeling is not easy due to the scarcity of experimental data in saturation conditions. For this purpose, it was proposed to first obtain experimental data for the compounds used, whose modeling would permit extrapolation to saturation conditions, minimizing the influence of errors of $v_i^o(T)$ on the calculation of the $\gamma_i(p, T, x_i, y_i)$ of the iso-p VLE. For the six compounds of this work, densities were measured at different pressures, $p \in [0.1-40]$ MPa, and temperatures, $T \in [278.15-418.15]$ K, and are recorded in Table S4. The literature[34−43] contains values of (p, ρ, T) for the saturated hydrocarbons, and the comparison with our data is shown in Figure S2 (SI), revealing percentage errors lower than 0.3%, validating the experimentation performed. However, no data were found for esters, with original data presented in Table S4. To obtain a greater precision in the estimation of $v_i^o(T)$, the use of new modeling was analyzed, the development of which is presented in the following section.

3.1.2.1. Selection of a Model to Estimate Molar Volumes of Pure Compounds at Saturation. Values of $p-\rho-T$ collected in Table S4 for each compound were first correlated with the Tait equation, eqs 4 and 5. Parameters A_i, B_i, and C_i were optimized by nonlinear regression,[28] minimizing the objective function RMSE = $s(\rho_i)$, given by eq 6; numerical values of the coefficients and statistical parameters are shown in Table S5. In Figure S2, the deviations between our data and those obtained from the literature are compared.

$$\text{ARD} = \frac{1}{m_\rho} \sum_{j=1}^{m_\rho} \left|\frac{\rho_{j,\text{exp}} - \rho_{j,\text{cal}}}{\rho_{j,\text{exp}}}\right| \times 100,$$

$$\text{RMSE} = \left[\sum_{j=1}^{m_\rho} (\rho_{i,j,\text{exp}} - \rho_{i,j,\text{cal}})^2/(m_\rho - 1)\right]^{0.5} \tag{6}$$

Moreover, Figure S3 shows the RSME vs T/K of the values obtained with eq 6. Two regions of minimum error are observed, one at low temperature ($\approx$300 K) and another at high temperature ($\approx$415 K). The latter behavior could be a consequence of a "Runge effect" caused using polynomial expressions, as eq 5, to fit the reference densities. The VLE experiments were carried out within the interval $T \in (400 \pm £)$; therefore, it was deemed appropriate to use another equation that provides a better representation of the $v_i^o(T)$ for the compounds studied. A correlation was performed using a method proposed by Ihmels and Gmehling,[44] combining the Tait equation, in the form of eq 4, with the Rackett equation, which provides values corresponding to the reference state, that is, the values of $\rho_{i,0}(T, p_0)$ for the liquid saturated at the temperature of the system at VLE. The Rackett equation, written logarithmically, is

$$\ln \rho_i^o(T) = \ln \hat{a} - [1 + (1 - T/\hat{c})^{\hat{d}}]\ln \hat{b} \tag{7}$$

The results obtained with the combined model are recorded in Table 2. A comparison of the statistics used to quantify the quality of fit, ARD and RMSE, reflects a better behavior for this second procedure in relation to the Tait equation. Figure 5 shows the profile offered by the different equations (Tait, Rackett, and combined) in the interval of values measured for each compound, and special attention should be paid to the interval of temperatures corresponding to the iso-p VLE presented here. Zooming in on the part of this interval shows that the method employed here produces slightly better results than the other two equations used individually.

3.2. Solutions. *3.2.1. Volumetric and Energetic Effects in the Mixing Process.* The values (x_1, T, ρ, v^E) obtained for each of the binaries $H_5C_2COOC_vH_{2v+1}$ ($v = 3, 4$) + C_nH_{2n+2} ($n = 6-9$) are shown in Table S6. As indicated in Section 2.2, the direct measurements (x_1, ρ) at $T = 298.15$ K of the corresponding binaries are represented by eq 1, used to describe the compositions of the iso-p VLE (Table S7). The v^Es of the set, calculated at different temperatures, are represented in Figure 5 and reveal a quasiregular increase with n but decrease, for a given alkane, with the increase in
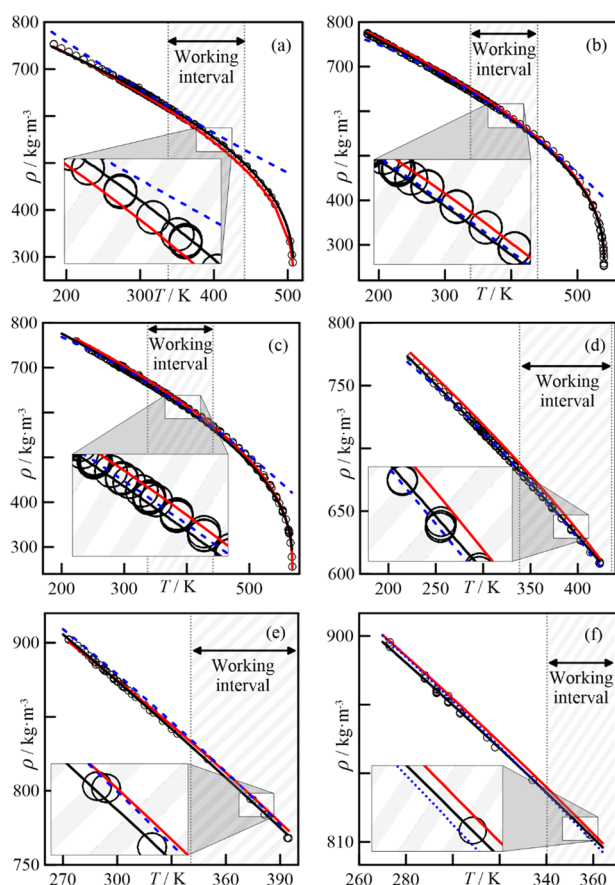
Figure 5. Comparison of saturation densities calculated using different equations and experimental values. (Open thick black circles) literature data, (solid black lines) combined Tait's equation, (dashed blue lines) original Tait's equation, and (solid red lines) Rackett's equation. (a) hexane, (b) heptane, (c) octane, (d) nonane, (e) propyl propanoate, and (f) butyl propanoate.


Figure 6. Experimental excess molar properties, h^E and pv^E, obtained for (a) propyl propanoate+alkane and (b) butyl propanoate + alkane. (Open black circles) pv^E at T = 298.15 K (thick black crosses), pv^E at T = 308.15 K, (open red circles) h^E at T = 298.15 K, and (thick red crosses) h^E at T = 308.15 K. Curves were obtained with the model described and parameters of Table 3.

3.2.2. Results of the Vapor−Liquid Equilibria. The iso-p VLE data of the eight systems (T, x_1, y_1) were obtained following the experimental methodology described in Section 2.2. The numerical information is compiled in Table S9, while, graphically, the T vs x_1,y_1 values of all binaries with propyl and butyl propanoate are shown in Figure 7, and those of ($y_1 - x_1$)
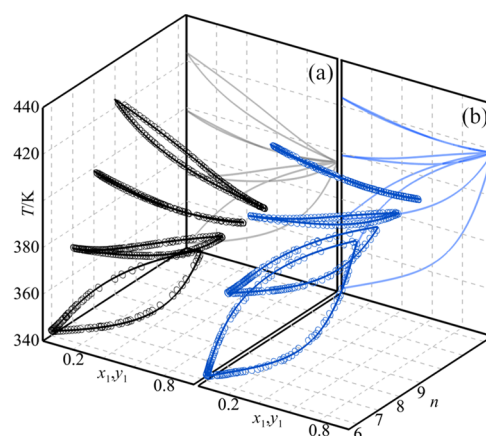
Figure 7. T, x, y diagrams for the so-p VLE of (open black circles) propyl propanoate + alkane and (open blue circles) butyl propanoate + alkane. Curves were obtained with the model described and parameters of Table 3.

ester size. The effect of temperature on the v^Es depends on the hydrocarbon present. The solutions with heptane, octane, and nonane present an expansive effect, $(\partial v^E/\partial T)_{p,x} > 0$, as empty spaces are created in the final solution, with this effect reversing $(\partial v^E/\partial T)_{p,x} < 0$ with the hexane. Figure S4 shows the comparison between values obtained for this work and those available in the literature.[1,2,4,5,7]

On the other hand, the experimental h^E values for the binaries (propyl or butyl propanoate) + (C_6, C_8) (T = 298.15 and 318.15 K) obtained are recorded in Table S8 (SI) and are represented in Figure 6, as the h^E of the other mixtures were taken from previous studies.[2,5−7] All binaries are endothermic, $h^E > 0$, with the values increasing with n and decreasing with v. The increase in temperature has a little effect on the mixing energies, producing quasinegative slopes. Figure S5 shows representations of $h^E = h^E(x)$ for the experimental values and those from the literature,[2,3,5,7] which have been used in the modeling process, as shown in Table S1. In brief, the mixing effects, using v^E and h^E, confirm observations made in previous studies[5,6] about the proposed model for these solutions. Two types of interactions are considered mainly, those of Van der Waals, evaluated as contact surfaces between aliphatic portions, and dipole−dipole interactions, evaluated as dipolar moments of the esters, with the latter decreasing as a consequence of the mixing process at the expense of the former.

vs x_1 in Figure 8, while the individuals are shown in Figures S6 and S7. Figure S6b,d compare the experimental results obtained in this work with other results published recently by our group[4] for the systems propyl propanoate (1) + heptane (2) or nonane (2), respectively. Slight differences are observed between the data series, justified by the different quality of the chemicals used.

Two of the systems, propyl propanoate(1) + octane(2) (0.585; 392.9) and butyl propanoate(1) + nonane(2) (0.633; 417.1), are azeotropic at the coordinates ($x_{1,az}$;T_{az}/K). The activity coefficients for each compound, γ_i, were calculated with the $\gamma-\varphi$ method by
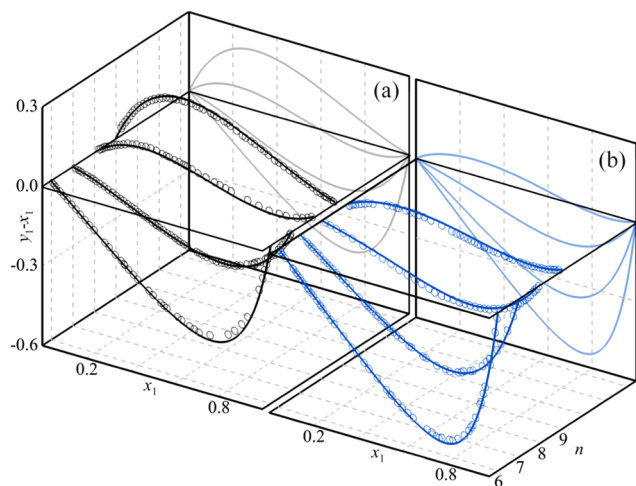
Figure 8. Diagrams of $(y - x)$ vs x,y for the iso-p VLE of (open black circles) propyl propanoate+alkane and (open blue circles) butyl propanoate + alkane. Curves were obtained with the model described and parameters of Table 3.

$$\gamma_i(x_i, p, T) = \frac{py_i}{x_i p_i^o} \Phi_i(p, T, y_i)$$

$$= \frac{py_i}{x_i p_i^o} \exp\left[\frac{(B_{ii} - v_i^o)(p - p_i^o) + (2B_{ij} - B_{ii} - B_{jj})py_{j\neq i}^2}{RT}\right] \tag{8}$$

The p_i^o values at each T were calculated with the Antoine equation and parameters for the esters in Table 1 and those corresponding to the hydrocarbons in the literature;[25,27] the virial coefficients, B_{ij} $(i,j = 1, 2)$, were estimated with the Tsonopoulos proposal[45] and the $v_i^o(T)$ with the combined Tait–Rackett equation and the parameters of Table 2. The values of γ_i are presented in Table S9 together with those corresponding to excess Gibbs energy in its adimensional form $g^E/RT = \sum_1^2 x_i \ln \gamma_i$.

4. THERMODYNAMIC–MATHEMATICAL TREATMENT OF THE EXPERIMENTAL INFORMATION. NEW CONTRIBUTION TO MODELING–CHECKING TASKS

According to the diagram in Figure 1, the dense experimental information collected for this work is submitted to analytical representations (modeling) and thermodynamic verification (checking). In addition, some modifications are proposed below for both tasks to obtain the best results.

4.1. Modeling. The simultaneous/combined modeling of the experimental information, iso-p VLE and mixing properties, $v^E = v^E(x)$ and $h^E(x)$, was carried out with the semi-empirical model already used,[10] written for the excess Gibbs energy, g^E, as

$$g^E = z_1 z_2 \sum_{j=0}^{N} g_j(p, T) z_1^j \quad \text{with} \quad z_1 = \frac{x_1}{x_1 + k_g x_2} \tag{9}$$

where $g_j = g_j(p, T)$. In previous studies,[10,11] this coefficient was used as the sum of the terms containing five coefficients assigned to monomials of the type $(p, p^2, 1/T, T, T^2)$. However, for this model to be extended to other thermodynamic quantities, such as volumes, a logarithmic term has been introduced, which arises from the integration of c_p^E values, with the new expression being

$$g_j = g_{j0} + g_{j1}p^2 + g_{j2}p \ln T + g_{j3}T + \frac{g_{j4}}{T} + g_{j5}T^2 \tag{10}$$

The following expressions are obtained now for different quantities, γ_1, h^E, and v^E

$$RT \ln \gamma_i = z_1 z_2 \sum_{j=0}^{N} g_j z_1^j + \left[\frac{(2 - x_1 + i)k_g z_1^2}{x_1^2}\right] \sum_{j=0}^{N+1} (j + 1)(g_j - g_{j-1})z_1^j$$

$$\text{with} \quad g_{-1} = g_{N+1} = 0 \tag{11}$$

$$h^E = z_1 z_2 \sum_{j=0}^{N} \left[g_{j0} + g_{j1}p^2 + g_{j2}p(\ln T - 1) + \frac{2g_{j4}}{T} - g_{j5}T^2\right]z_1^j;$$

$$v^E = z_1 z_2 \sum_{j=0}^{N} [2g_{j1}p + g_{j2}\ln T]z_1^j \tag{12}$$

This achieves a single model to represent the different available properties of a system; therefore, the next task is to achieve a complete definition or an appropriate parametrization of the model (including the parameters k_g and g_{jk}), which constitutes a multiobjective problem. This problem was solved using a procedure already proposed,[14] which selects the minimum number of parameters for eq 10 necessary to model the behavior of the systems, avoiding the overfitting in the resulting model. The efficient-solutions front (i.e., non-dominated) is constructed using the ε-constraint method,[46] decomposing the global multiobjective problem into a sequence of restricted mono-objective problems, where, in each of these, the error made by the model is minimized when reproducing

(a) The iso-p VLE data, quantified by the particular objective function

$$f_\gamma(\boldsymbol{\theta}) = \sum_{q=1}^{m_{\text{VLE}}} \sum_{i=1}^{2} x_{iq} \cdot [\gamma_{i,q,\text{exp}} - \gamma_{i,q,\text{cal}}(\boldsymbol{\theta})]^2 / 2m_{\text{VLE}} \tag{13}$$

where x_{iq} is the molar fraction at each point, acting as the weighting coefficient of the error of γ_I.

(b) The objective function associated with the error of h^E

$$f_h(\boldsymbol{\theta}) = \left[\sum_{q=1}^{m_h} (h_{q,\text{exp}}^E - h_{q,\text{cal}}^E(\boldsymbol{\theta}))^2 / (m_h - 1)\right]^{1/2} \tag{14}$$

(c) The objective function associated with the error of v^E

$$f_v(\boldsymbol{\theta}) = \left[\sum_{q=1}^{m_v} (v_{q,\text{exp}}^E - v_{q,\text{cal}}^E(\boldsymbol{\theta}))^2 / (m_v - 1)\right]^{1/2} \tag{15}$$

where $\boldsymbol{\theta} = \{g_{00},..., g_{jk},..., g_{N5}, k_{21}\}$ is the vector of the model parameters. These two last particular objective functions are formulated as restrictions of the problem, establishing different maximum values, ε_h and ε_v, in the intervals: $\varepsilon_h \in [5,50]$ J·mol^{-1} and $\varepsilon_v \in [5,50]$ 10^9 m^3·mol^{-1}. The best model parameters for each system are selected with a vector of binary variables, $\mathbf{a} = \{a_{00},..., a_{jk},..., a_{N5}\}$ each of which is associated with one of the g_{jk}. In this way, each of the particular mono-objective problems is formulated as mixed integer nonlinear programming (known as the mixed integer nonlinear problem (MINLP) procedure). Finally, to consider the precision and complexity of the model simultaneously in the optimization

Table 3. Parameters of Equations 9 and 10 Obtained for the Combined Modeling of iso-p VLE, h^E, and v^E Data of the Systems Propyl or Butyl Propanoate(1) + (Hexane–Nonane)^a

	propyl propanoate					butyl propanoate				
	hexane	heptane	octane^{R1}	octane^{R2}	nonane	hexane	heptane	octane^{R1}	octane^{R2}	nonane
g_{00}	3.1160×10^3	3.3521×10^3	3.3981×10^3	-3.0659×10^2	3.0163×10^3	3.2574×10^3	3.4312×10^3	3.3914×10^3	3.4312×10^3	2.8074×10^3
g_{01}	1.0021×10^{-11}	-2.0428×10^{-11}	4.5214×10^{-12}	1.3611×10^{-11}	-5.0980×10^{-12}	5.5644×10^{-11}	1.2573×10^{-11}	-7.7097×10^{-11}	1.2573×10^{-11}	1.1949×10^{-11}
g_{02}	-7.6746×10^{-8}	1.1332×10^{-6}	3.0140×10^{-7}	3.6459×10^{-8}	8.0700×10^{-7}	-1.7862×10^{-6}	-1.3663×10^{-7}	3.1893×10^{-6}	-1.3663×10^{-7}	-4.1378×10^{-8}
g_{03}	-5.6979	-5.2193	-5.8382	1.0193×10	1.2900	-4.0533	-5.6219	-4.0322	-5.6219	-3.0552
g_{04}	1.4931×10^4	–	-5.0792×10^4	2.9718×10^5	–	-3.0646×10^4	–	-7.2690×10^4	–	–
g_{05}	1.6145×10^{-3}	-4.2721×10^{-4}	-8.2036×10^{-4}	-1.9258×10^{-2}	-1.2093×10^{-2}	-6.6723×10^{-5}	–	-4.3762×10^{-3}	–	-3.3965×10^{-3}
g_{10}	–	–	2.9420×10^2	–	–	–	6.8326×10	5.1896×10^2	6.8326×10	–
g_{11}	-5.1588×10^{-11}	-1.5003×10^{-10}	-3.5771×10^{-10}	-4.1090×10^{-10}	-3.5920×10^{-10}	4.2154×10^{-11}	$-1.1573\text{E-}10$	-7.6990×10^{-11}	-1.1573×10^{-10}	-2.4504×10^{-10}
g_{12}	1.7686×10^{-6}	5.2623×10^{-6}	1.2649×10^{-5}	–	1.2477×10^{-5}	-1.8192×10^{-6}	3.9516×10^{-6}	2.4422×10^{-6}	3.9516×10^{-6}	8.6954×10^{-6}
g_{13}	-2.1258	–	6.0602	–	–	–	1.8886	–	1.8886	–
g_{14}	–	-3.6209×10^4	–	–	–	–	-2.1686×10^5	–	-2.1686×10^5	–
g_{15}	7.2856×10^{-3}	–	-6.8328×10^{-3}	–	–	–	–	–	–	–
g_{20}	–	–	8.2442×10^2	–	–	–	1.3315×10^3	-9.8248×10^2	1.3315×10^3	–
g_{21}	3.8092×10^{-11}	1.7012×10^{-10}	3.0707×10^{-10}	3.6412×10^{-10}	3.3383×10^{-10}	1.2250×10^{-11}	2.0543×10^{-11}	1.9816×10^{-10}	2.0543×10^{-11}	7.8271×10^{-11}
g_{22}	-1.3432×10^{-6}	-5.9748×10^{-6}	-1.0751×10^{-5}	-1.2778×10^{-5}	-1.1660×10^{-5}	-2.6620×10^{-7}	-6.8850×10^{-7}	-6.8624×10^{-6}	-6.8850×10^{-7}	-2.6615×10^{-6}
g_{23}	–	6.6556	-4.7639	–	–	–	-3.4852	1.9868	-3.4852	8.8929
g_{24}	3.1975×10^5	–	–	–	–	-2.0024×10^5	–	–	–	–
g_{25}	–	-1.3507×10^{-2}	–	–	–	–	–	–	–	-1.5929×10^{-2}
k_{12}	6.8155×10^{-1}	7.9215×10^{-1}	8.0730×10^{-1}	9.1033×10^{-1}	1.0491	1.0794	8.5479×10^{-1}	1.0054	8.5479×10^{-1}	7.4323×10^{-1}
$s(g^E/RT)$	0.004	0.005	0.011	0.007	0.009	0.013	0.006	0.005	0.002	0.002
$s(\gamma_i)$	0.081	0.023	0.109	0.038	0.047	0.091	0.063	0.045	0.040	0.065
$s(h^E)$	17	6	16	15	10	14	7	7	8	6
$s(v^E)$	6	11	9	10	9	8	14	8	8	13

^{a}"—" Parameters discarded, R1: using VLE data obtained in run 1, R2: using VLE data obtained in run 2.

process, the Akaike information criterion[47,48] is used, corrected for small samples, which adopts the form

$$\mathrm{AIC}(\boldsymbol{\theta}, \mathbf{a}) = m_{\mathrm{VLE}}(\log(2\pi/m_{\mathrm{VLE}}) + \log f_\gamma(\boldsymbol{\theta}) + 1) + 2K,$$

$$\mathrm{AIC}_c = \mathrm{AIC} + \frac{2K(K+1)}{N-K+1} \tag{16}$$

The variable K is the number of parameters and represents the complexity of the model. It is modified as explained earlier[14] to favor parameters of a lower order in the polynomial established for eq 10, as follows

$$K = \sum_{j=0}^{N-2} \sum_{k=0}^{5} \left(\left\lfloor \frac{6j+k}{6} \right\rfloor + 1 \right) \cdot a_{jk} \tag{17}$$

In summary, the formulation represented by the following scheme 18 describes the optimization problem addressed in this step, whose resolution was performed with a genetic algorithm (GA), described in a previous work,[14] the programming of which was implemented in R language, using the GA extension package.[49,50] From the efficient-solutions front of each system, the model that adequately represents all of the measured quantities for the dissolutions of this work was finally selected.

$$\min_{\boldsymbol{\theta}, \mathbf{a}} \mathrm{AIC}_c(f_\gamma(\boldsymbol{\theta}))$$

$$\text{s. t. } f_h(\boldsymbol{\theta}) \le \varepsilon_h$$

$$f_v(\boldsymbol{\theta}) \le \varepsilon_v$$

$$-g_{00}^u a_{00} \le g_{00} \le g_{00}^u a_{00}$$

$$\vdots$$

$$-g_{jk}^u a_{jk} \le g_{jk} \le g_{jk}^u a_{jk}$$

$$\vdots$$

$$-g_{N5}^u a_{N5} \le g_{N5} \le g_{N5}^u a_{N5}$$

$$\mathbf{a} \in \{0, 1\}^{6(N+1)} \tag{18}$$

The numerical values obtained in the simultaneous modeling of all of the properties, using an MINLP optimization procedure, are compiled in Table 3, and the graphical representations of the quantities are shown in Figures 6−8. For the differences observed in the representation of iso-p VLE data in binaries with octane, see Figures S6 and S7, although the modeling of h^E and v^E is acceptable (Figure 6).

4.2. Checking. The quality of the experimentation, from a thermodynamic point of view, was verified using a methodology designed previously[12] by applying several tests described in the literature. As we know in the VLE experimentation of binaries, four variables (p, T, x, y) are measured and the system is overdimensioned and therefore it is necessary to check these variables. In addition, the method proposed in previous studies,[13−15] based on the resolution of the Gibbs−Duhem equation, is also used, proposing here a modification to demand better data quality and scientific rigor. For a binary system, the differential of eq 8 is introduced in the Gibbs−Duhem equation, giving rise to[13]

$$\left[\frac{y_1 - x_1}{y_1(1 - y_1)} - \sum_{i=1}^{2} x_i \left(\frac{\partial \Phi_i}{\partial y_1} \right)_{T,p} \right] dy_1$$

$$= \left[\frac{h^E}{RT^2} - \sum_{i=1}^{2} x_i \frac{d\ln p_i^o}{dT} - \sum_{i=1}^{2} x_i \left(\frac{\partial \ln \Phi_i}{\partial T} \right)_{p,y} \right] dT \tag{19}$$

Therefore, the latter equation is also a form of the Gibbs−Duhem equation. Equation 19 is solved in two independent ways (integral and differential forms), thus verifying the dependency relationships between the variables measured. Both forms establish a rigorous method for checking the measured variables. A resolution method was previously proposed,[13] but some modifications are introduced in this work to standardize the quality evaluation indices for the different cases considered.

4.2.1. Integral Form. It corresponds to the numerical integration of eq 19, written as

$$dT = \frac{\left[\frac{y_1 - x_1}{y_1(1 - y_1)} - \sum_{i=1}^{2} x_i \left(\frac{\partial \Phi_i}{\partial y_1} \right)_{T,p} \right]}{\left[\frac{h^E}{RT^2} - \sum_{i=1}^{2} x_i \frac{d\ln p_i^o}{dT} - \sum_{i=1}^{2} x_i \left(\frac{\partial \ln \Phi_i}{\partial T} \right)_{p,y} \right]} dy_1 \tag{20}$$

This is used to obtain temperature values $T_{i,\mathrm{cal}}$, which correspond to reference values for experimental data i, $T_{i,\mathrm{exp}}$. A modification of the methodology used previously[13] is applied here; thus, a value is considered to be consistent if the difference between both is smaller than the maximum inconsistency permitted, $\varepsilon_{T,i}^M$, which is related to the combined uncertainty, $u_{T,i}$, of the temperature as

$$\hat{T}_i = \varepsilon_{T,i}^M - |T_{i,\mathrm{exp}} - T_{i,\mathrm{cal}}| \quad \text{being} \quad \varepsilon_{T,i}^M = \kappa_T u_{T,i} \tag{21}$$

by a "coverage factor" κ_T whose value should be previously established according to the quality requirement. For binary systems, it is sufficient to use $\kappa_T = 3$ to prevent the appearance of false positives in the data evaluation. In summary, an inconsistency criterion for point-to-point data evaluation is proposed by the difference shown by eq 21. This particular criterion of each point can be extended to all VLE values, that is, the integral form verifies the data consistency if $\overline{\delta \hat{T}} > 0$ for a series of N VLE data, such that

$$\overline{\delta \hat{T}} = \sum_{i=1}^{N_{\mathrm{VLE}}} \hat{T}_i / N_{\mathrm{VLE}} > 0 \tag{22}$$

4.2.2. Differential Form. The differential eq 19 can also be rewritten, separating the terms containing the experimental data alone, defining a parameter $\zeta_{i,\mathrm{exp}}$, from those that require a mathematical model, the second term of that equation.

$$\zeta_{i,\mathrm{exp}} = \frac{y_{1,i} - x_{1,i}}{y_{1,i}(1 - y_{1,i})} = \sum_{i=1}^{2} x_i \left(\frac{\partial \Phi_i}{\partial y_{1,i}} \right)_{T,p} \tag{23}$$

If the experimental data are identical to those generated by the model, then $\zeta_{i,\mathrm{cal}} = \zeta_{i,\mathrm{exp}}$. It has been proposed that the difference between both quantities represents the consistency of the set {data + model}, which should be less than the maximum inconsistency permitted, $\varepsilon_{\zeta,i}^M$; therefore, following a similar approach to the above, for a point i

Table 4. Results of the Consistency Tests Used to Validate iso-p VLE Data^a

	areas		Fredenslund		direct		Wisniak		Kojima			proposed test		
												integral form	differential form	
system	D_A	R	δy	R	$\delta \ln(\gamma_1/\gamma_2)$	R	D_w	R	I1	I2	R	$\overline{\delta \hat{T}}$	$\overline{\delta \hat{\zeta}}$	R
					Propyl Propanoate(1)+									
hexane(2)	0.27	rej.	0.007	app.	0.087	app.	3.9	app.	7.7	105.4	rej.	0.05	0.04	app.
heptane(2)	0.13	rej.	0.005	app.	0.045	app.	3.1	app.	10.8	31.3	rej.	0.06	0.15	app.
octane(2)$^{run\ 1}$	0.04	rej.	0.004	app.	0.030	app.	2.6	app.	31.1	9.1	rej.	−0.02	0.03	rej.
octane(2)$^{run\ 2}$	0.15	rej.	0.006	app.	0.041	app.	2.6	app.	13.2	24.9	app.	0.01	0.04	app.
nonane(2)	0.07	rej.	0.006	app.	0.012	app.	3.7	app.	54.2	4.3	rej.	0.04	0.01	app.
					Butyl Propanoate(1)+									
hexane(2)	0.13	rej.	0.001	app.	0.014	app.	4.2	app.	21.5	8.8	app.	0.15	0.16	app.
heptane(2)	0.05	rej.	0.002	app.	0.005	app.	3.5	app.	9.9	11.7	app.	0.12	0.05	app.
octane(2)$^{run\ 1}$	0.36	rej.	0.009	app.	0.059	app.	3.0	app.	21.7	84.6	rej.	−0.08	−0.01	rej.
octane(2)$^{run\ 2}$	0.17	rej.	0.004	app.	0.058	app.	2.9	app.	2.3	8.7	app.	0.07	0.11	app.
nonane(2)	0.31	rej.	0.008	app.	0.053	app.	3.2	app.	21.2	20.4	app.	0.02	0.02	app.

^{a}R: result; rej.: rejected data set; app.: approved data set; R1: data set in run 1; R2: data set in run 2.

$$\hat{\zeta}_i = \varepsilon^M_{\zeta,i} - |\zeta_{i,\exp} - \zeta_{i,\text{cal}}| \quad \text{where} \quad \varepsilon^M_{\zeta,i} = \kappa_\zeta u_{\zeta,i} = 3u_{\zeta,i}$$

(24)

This parameter measures the point-to-point consistency according to the differential form of the test and where $u_{\zeta,i}$ is the combined uncertainty of $\zeta_{i,\exp}$. The *cov*erage parameter, which has a value of 3, is sufficient for this case. Likewise, the mean value for eq 24 is a global measure of consistency, in accordance with the differential form.

$$\overline{\delta \hat{\zeta}} = \sum_{i=1}^{N_{\text{VLE}}} \hat{\zeta}_i / N_{\text{VLE}} > 0$$

(25)

In brief, for a set of iso-p VLE to be thermodynamically validated, $\overline{\delta \hat{T}} > 0$ and $\overline{\delta \hat{\zeta}} > 0$ must be obeyed. Table 4 shows the results of the different methods/tests of consistency, taking into account the recommendations made in a previous article.[12] This can be summarized as follows:

1. The eight systems are rejected with the areas' test but are consistent with the Fredenslund, direct Van Ness, and Wisniak tests.

2. The Kojima method rejects five systems, including those containing octane, which are also rejected by the test proposed above.

This result suggests repeating the iso-p VLE measurements for the solutions with octane. The new values (recorded as run 2) are shown in Table S9 and graphically in Figure 9. The new data series for the binaries $H_5C_2COOC_\nu H_{2\nu+1}$ (ν = 3,4) + C_8H_{18} are modeled using the above-described procedure in Section 4.1, with the new parameterization shown in Table 3, revealing a qualitative improvement in the representation of iso-p VLE values, γ_i and g^E/RT (Figure 9). The new series gave positive results with the different consistency tests, see Table 4, and now, the series named run 2 is validated by all of the tests, except by the areas' test, but, despite this, it shows to be a more reliable data set, recommending its use. After receiving the positive evaluation of the model-checking binomial for the iso-p VLE data, additional information characteristic of each solution is obtained, i.e., the new situation of the azeotrope for propyl propanoate(1) + octane(2) in ($x_{1,az}$ = 0.650; T_{az}/K = 392.4).
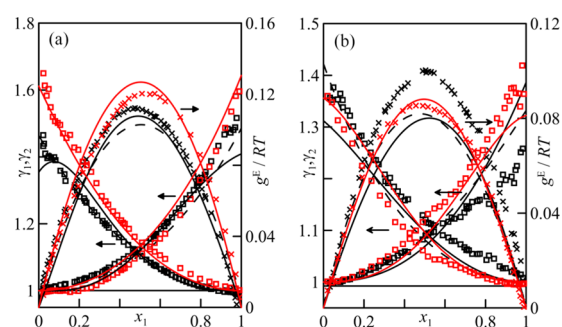

Figure 9. Representation of calculated values of γ_i vs x_1 (run 1: open thick black squares; run 2: open thick red squares) and g^E/RT vs x_1 (run 1: thick black crosses; run 2: thick red crosses) for (a) propyl propanoate(1) + octane(2) and (b) butyl propanoate(1) + octane(2). The curves were obtained using eq 9 and the parameters of Table 3 for the data series obtained in the (solid black lines) run 1 and (solid red lines) run 2 (dashed black lines) UNIFAC.[52]

5. BATCH-DISTILLATION PROCESS: SIMULATION AND EXPERIMENTATION

The stage-based methodology that supports the development of this work requires the simulation of a separation process for one of the binaries. The specific tool *BatchSep* from Aspen Plus[51] was employed to obtain information of the distillation of a solution, using the results emitted by a predictive method, i.e., UNIFAC.[52] Coherence between the simulation data and those obtained in the actual process depends on two factors: (i) the ability of the simulator to correctly reproduce the hydrodynamic and thermodynamic behavior of a distillation column and (ii) the analogy/discrepancy between the predicted VLE data and those obtained by experimentation and/or correlation. However, these items will not condition the functioning of a real distillation process, conducted on a pilot or larger scale; on the contrary, the information generated could influence other operation stages (see Figure 1).

For this work, the azeotropic binary propyl propanoate–octane was selected, which has a complex separation and presents certain discrepancies between experimental values/correlations of iso-p VLE and those estimated by UNIFAC (see Figure 10). For this purpose, the simulation generates results based on the modeling used by (a) NRTL using
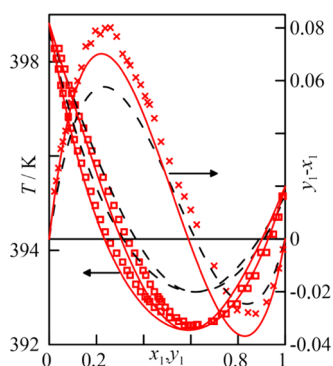
Figure 10. Plot of T vs x,y and $(y − x)$ vs x,y for the propyl propanoate(1) + octane(2) system. (Open thick red squares, thick red crosses) Experimental values; (solid red lines) the multiproperty modeling; (dashed black lines) UNIFAC.[52]

exclusively iso-p VLE data generated by UNIFAC and (b) the multiproperty modeling performed as described in Section 4.1 of this manuscript, using real data. On the other hand, the separation in a batch-distillation process is experimentally tested using the procedure described and the laboratory column shown in Figure 4.

The experiment was conducted in the column described in Section 2.2. The distillation flask was filled with ≈157 g of a mixture of propyl propanoate (1) + octane(2), $x_1 ≈ 0.28$, and the distillation was initialized at total reflux to reach the stationary state, starting the separation process with $r = 6$, with a duration of approximately 3 h. Samples of the distillate stream and bottom were taken at regular intervals, and the respective compositions, $x_{1,D}$ and $x_{1,B}$, were determined. The temperature of the distillate was recorded at regular intervals during distillation. Figure 11 shows an outline of the process.
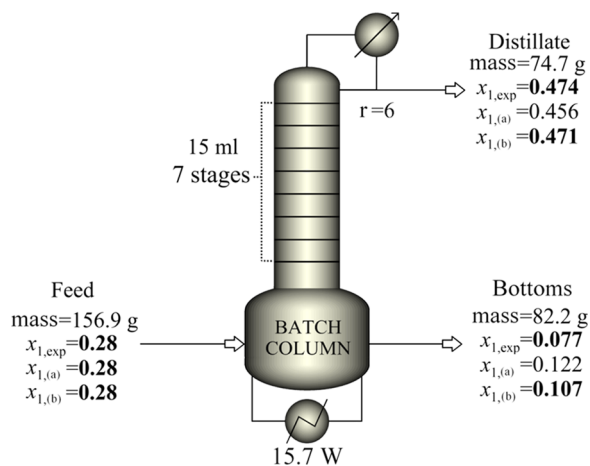
Figure 11. Scheme of a batch-distillation process shown by the simulator operating for the binary propyl propanoate(1) + octane(2). r, reflux ratio; exp, experimental; case (a); case (b).

The results of the two versions of the simulation processes were evaluated, considering relevant factors in a batch-distillation process: composition and temperature profiles over time and the quantities of material and compositions obtained from the distillate and the bottom stream at the end of the operation.

Figure 11 shows the compositions obtained (distillate and bottom fractions) in the batch distillation, both experimental

and that of the two simulation processes mentioned. In the simulator, quantities of the distillate and bottom fractions were set to constant values that coincided with values obtained experimentally. Hence, the simulator generated different composition values for cases (a) and (b), with the values of case (b) being closer to the real ones. The estimation made in case (a) (with VLE data predicted by UNIFAC) presents differences in the distillate compositions and bottom stream, $δx_D ≈ 0.02$; $δx_B ≈ 0.05$, while for case (b) (with multiproperty modeling), the differences are smaller: $δx_D ≈ 0.003$; $δx_B ≈ 0.03$.

5.1. Results of the Composition and Temperature Profiles Produced by the Simulator. Figure 12 shows the
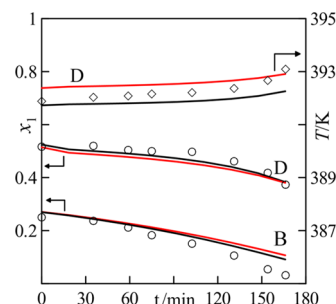
Figure 12. Profiles of composition and temperature obtained in the batch-distillation process of the solution propyl propanoate(1) + octane(2): (open black circles) experimental compositions, (open black rhombuses) distillate experimental temperatures, (solid black lines) case (b), and (solid red lines) case (a). D, distillate; B: bottom stream.

different composition and temperature profiles generated by the simulator for cases (a) and (b). The composition profiles of both cases are similar to experimental ones, presenting, respectively, differences for the distillate and residue in case (b) of 0.018 and 0.030; for case (a), the differences are 0.030 and 0.038, respectively. The values for the temperature profile of the distillate are also reproduced acceptably for the two cases, with mean differences of 0.38 and 0.33 K for (a) and (b), respectively. In summary, estimation of the temperature profile for case (b) (using the modeling proposed in this work) is similar to the experimental values for the column, during almost the entire operation time, except for the last 30 min.

From this, it is possible to deduce the influence of the modeling on the simulation of the separation process of the chosen solution. A conclusion is that the case presented as (b), with multiproperty modeling, reproduces better the corresponding experimental compositions of distillate and bottom fractions. This occurs in spite of the fact that the model loses some capacity to estimate a given property when an extended model has been achieved with simultaneous representation of several properties of the same system.

6. CONCLUSIONS

This work applies a sequential methodology, which we have named EMTS, to eight systems composed of two alkyl (propyl, butyl) propanoates and four alkanes (hexane to nonane). The Experimental Information provided in the Supporting Information contains almost 2500 original values of several properties: those that define the dilution effects (h^E and v^E) and the iso-p VLE of the binaries constituting the above compounds. The measurements for the mixing properties are

in good agreement with those in the literature, with the average errors ranging between 1 and 6% (see Figure 6). These results show that the physicochemical behavior of the systems confirms the structural model proposed previously, which can be partially extendible to other systems of polar/nonpolar components. Values obtained for iso-p VLE presented inconsistencies in the binaries containing octane and, therefore, new quality values (run 2) were measured.

To improve the calculations of the activity coefficients γ_{i}, several actions were carried out: (1) New vapor pressures were measured for alkyl propanoates, which showed maximum deviations of 0.8 and 5.5% for the corresponding propyl and butyl alkanoates, respectively, (2) for the two propanoates, original $p-\rho-T$ values were obtained, since there is no information for those esters in the literature; however, new values for the hydrocarbons were also measured, showing errors below 0.3% in relation to published data,[33−42] and (3) with the $p-\rho-T$ database generated, the evaluation of the molar volumes of pure compounds at saturation $v_{i}^{o}(T)$ was improved using a combined form of the Tait−Rackett equations (see eqs 4 and 7). This improvement allowed a theoretically more robust calculation of the activity coefficients through the $\gamma-\phi$ formulation for VLE data.

Implementation of a multiproperty modeling process addressed with a multiobjective optimization method was made, combining an objective function based on the Akaike information criterion with an MINLP genetic algorithm, to obtain the best modeling with the least number of parameters. A modified version of the model on g^{E}, eq 10, was used, improving the multifunctional correlation in relation to that used in previous studies. Thus, all properties were acceptably described using the thermodynamic formalism, with the average errors of the h^{E} and v^{E}, respectively, being less than 2 and 6% for the set of systems. The description of the VLE is also satisfactory with relative deviations of less than 9% in all cases. Another novelty introduced in this work is referred to as the thermodynamic checking of the experimental VLE data. Our own method was modified to improve its application, considering a greater restriction in the κ-parameter (eqs 21 and 24). The use of this more strict criterion caused the VLE of the two systems containing octane to be experimentally redetermined, obtaining a new series (run 2) of better-quality data, which were validated by the proposed method.[13] In relation to the verification procedure proposed, as deduced in Section 4.2, the general recommendation is to use the lowest possible value for κ to ensure a lesser uncertainty propagation to subsequent calculations. In other words, considering the {model-checking} binomial, according to Figure 1, the thermodynamic formalism described was used for all of the systems and the quality of the data employed in the procedure, especially the iso-p VLE, was verified.

The practical application of the EMTS tasks was performed on the azeotropic binary propyl propanoate−octane. Separation of the solution was proposed after establishing certain initial hypotheses, and a process simulation was carried out using the Aspen Plus simulator. On the one hand, the simulation using the estimations made by UNIFAC (simulator's own) was carried out; on the other hand, the modeling described in this work was used. Simultaneously, the operation of the batch-distillation column was performed in the laboratory (see Figure 4) to compare the efficacy of the procedure with real experimentation. The error produced by the simulator (using its own modeling) was 6 times greater

than that using our modeling in reproducing the distillate composition and 1.5 times greater for the bottom composition. When reproducing the composition profiles over time, the average percentage deviation of the simulator model was 1.7 times greater than when the proposed model was implemented. In summary, these results showed that the modeling performed with real iso-p VLE data, implemented in the simulator, produced values closer to experimental ones than the results generated with its own software, demonstrating a greater reliability for process simulation.

■ ASSOCIATED CONTENT

Ⓢ Supporting Information

The Supporting Information is available free of charge at https://pubs.acs.org/doi/10.1021/acs.iecr.0c00850.

> Background on the solutions propyl and butyl propanoate + alkanes. Experimental values corresponding to the characteristics of pure compounds, vapor pressures, $p-\rho-T$ values, excess properties, and iso-p VLE data. Errors between the values obtained in this work and those from the literature for vapor pressures, $p-\rho-T$, excess properties, and iso-p VLE data (PDF)

■ AUTHOR INFORMATION

Corresponding Author

Juan Ortega − *Grupo de Ingeniería Térmica e Instrumentación (IDeTIC), Parque Científico-Tecnológico, Universidad de Las Palmas de Gran Canaria, 35071 Las Palmas deGran Canaria, Canary Islands, Spain;* ● orcid.org/0000-0002-8304-2171; Email: juan.ortega@ulpgc.es

Authors

Luis Fernández − *Grupo de Ingeniería Térmica e Instrumentación (IDeTIC), Parque Científico-Tecnológico, Universidad de Las Palmas de Gran Canaria, 35071 Las Palmas deGran Canaria, Canary Islands, Spain*

Adriel Sosa − *Grupo de Ingeniería Térmica e Instrumentación (IDeTIC), Parque Científico-Tecnológico, Universidad de Las Palmas de Gran Canaria, 35071 Las Palmas deGran Canaria, Canary Islands, Spain*

Beatriz Lorenzo − *Grupo de Ingeniería Térmica e Instrumentación (IDeTIC), Parque Científico-Tecnológico, Universidad de Las Palmas de Gran Canaria, 35071 Las Palmas deGran Canaria, Canary Islands, Spain*

Raúl Ríos − *Grupo de Ingeniería Térmica e Instrumentación (IDeTIC), Parque Científico-Tecnológico, Universidad de Las Palmas de Gran Canaria, 35071 Las Palmas deGran Canaria, Canary Islands, Spain*

Jaime Wisniak − *Department of Chemical Engineering, Ben-Gurion University of the Negev, Beer-Sheva 84105, Israel*

Complete contact information is available at:
https://pubs.acs.org/10.1021/acs.iecr.0c00850

Notes

The authors declare no competing financial interest.

■ ACKNOWLEDGMENTS

■ NOMENCLATURE

General Symbols

AIC	Akaike information criteria
AIC_c	Akaike information criteria corrected for small samples
A,B,C	parameters of eq 2
a,b,c	parameters of the Antoine equation in reduced coordinates
$\mathbf{a}$	vector composed by the variables a_{jk}
B_{ii}	second virial coefficient of the pure compound i
B_{ij}	second virial coefficient of the mixture of compounds $i{-}j$
$e(p_i^o)$	error for p_i^o, $e(p_i^o) = 100(p_{i,exp}^o - p_{i,lit}^o)/p_{i,exp}^o$
f_γ	particular objective function for VLE, eq 13
f_h	particular objective function for excess enthalpy, eq 14
f_v	particular objective function for excess volume, eq 15
g^E	excess Gibbs energy of a solution, J·mol^{-1}
g_j	temperature- and pressure-dependent coefficient of the model, eq 9
g_{ij}	temperature- and pressure-independent coefficient of the model, eq 10
h^E	mixing enthalpy, J·mol^{-1}
iso-p	isobaric data set
iso-T	isothermal data set
K	parameter counter, eqs 16 and 17
k_g^{12}	parameter of eq 9
MINLP	mixed integer nonlinear problem
m	number of experimental data
m_{VLE}	number of experimental data of VLE
m_p	number of experimental data of vapor pressure
m_ρ	number of experimental data of density
m_h	number of experimental data of excess enthalpy
m_v	number of experimental data of excess volume
N	polynomial degree, eqs 11 and 12
n	number of compounds in a solution
n_D	refractive index
OF	multiobjective function
p	pressure, kPa
p_a	atmospheric pressure, $p_a \approx 98.9$ kPa
p_i^o	vapor pressure of the pure component i, kPa
$p_{r,i}^o$	reduced vapor pressure of the pure component i at certain temperature
q_i	surface parameter
$s(f)$	root-mean-square error of the function f
R	gas constant, J·mol^{-1}·K^{-1}
r_i	volumetric parameter
T	temperature, K
T_r	reduced temperature
T_i^o	normal boiling temperature of pure compound i, K
$\hat{T}_j$	quality of the function T_j for the point j, eq 21
$\overline{\delta T}$	average value of $\hat{T}_j$, eq 22
$u_{T,q}$	combined uncertainty of experimental temperature, eq 21
$u_{\zeta,q}$	combined uncertainty of the function ζ_I, eq 24
VLE	vapor−liquid equilibrium
v_i^o	saturated volume of the pure compound i, m^3·mol^{-1}
v_i^*	molar volume of pure compound i, m^3·mol^{-1}
v^E	excess molar volume of a mixture, m^3·mol^{-1}
x_i	mole fraction of compound i in the liquid phase
y_i	mole fraction of compound i in the vapor phase
w_i	generic mole fraction of compound i, $w_i = y_i$ or x_i
z_i	active fraction of the compound i, eq 9

■ GREEK LETTERS

α	expansion coefficient, K^{-1}
Δ	increment
δ_{ij}	relation of virial coefficients: $\delta_{ij} = 2\,B_{ij} - B_{ii} - B_{ii}$
δ_f	residue of the function f, $\delta_f = f_{exp} - f_{cal}$
$\varepsilon_h, \varepsilon_v$	maximum error admissible in a certain step of the ε-constraint procedure
ε_T^M	maximum admissible inconsistency on T, eq 21
ε_ζ^M	maximum admissible inconsistency on the function ζ, eq 24
γ_i	activity coefficient of the compound i
ρ	density in kg·m^{-3}
ρ_i	density of pure compound i in kg·m^{-3}
ρ_i^o	density of pure compound i at saturation in kg·m^{-3}
η	pseudorandom number
Φ_i	fugacity factor for the calculation of the activity coefficient, eq 4
$\boldsymbol{\theta}$	vector composed by the parameters of eqs 13−18
θ_i	parameters of eq 1
ψ	main variable in eq 19. For iso-p, $\psi = T$. For iso-T, $\psi = p$
ζ_{exp}, ζ_{cal}	functions defined by eq 23
ω	acentric factor

■ SUPER AND SUBINDICES

az	relative to an azeotrope
cal	calculated
exp	experimental data
i	index used to indicate a compound
j	index used to indicate a polynomial degree
q	index used to indicate an experimental data in a data series
o	property at saturated conditions
∞	infinite

■ REFERENCES

(1) Casas, H.; Segade, L.; Franjo, C.; Jiménez, E.; Paz-Andrade, M. I. Excess Properties for Propyl Propanoate+Hexane+Benzene at 298.15 K. *J. Chem. Eng. Data* **1998**, *43*, 756−762.

(2) Lorenzana, M. T.; Legido, J. L.; Jimenez, E.; Fernandez, J.; Pias, L.; Ortega, J.; Paz-Andrade, M. I. Thermodynamic Properties of (a Propyl Ester+an n-Alkane) at 298.15 K I. {$xC_2H_5CO_2C_3H_7$+(1-x)C_nH_{2n+2}}, (n = 6 to 10). *J. Chem. Thermodyn.* **1989**, *21*, 1017−1022.

(3) Casas, H.; Segade, L.; Franjo, C.; Jiménez, E.; Paz Andrade, M. I. Excess Molar Enthalpies of Propyl Propanoate+ Hexane+Benzene at 298.15 K and 308.15 K. *J. Chem. Eng. Data* **2000**, *45*, 445−449.

(4) Ortega, J.; Gonzalez, C.; Galvan, S. Vapor-Liquid Equilibria for Binary Systems Composed of a Propyl Ester (Ethanoate, Propanoate, Butanoate)+an n-Alkane (C_7, C_9). *J. Chem. Eng. Data* **2001**, *46*, 904−912.

(5) Ortega, J.; Vidal, M.; Toledo, F. J.; Placido, J. Thermodynamic Properties of (a Propyl Ester+an n-Alkane). XII. Excess Molar Enthalpies and Excess Molar Volumes for {$xCH_3(CH_2)_{u-1}COO$-$(CH_2)_2CH_3$ +(1-x)$CH_3(CH_2)_{2v+1}CH_3$} with u = 1 to 3, and v = 1 to 7. *J. Chem. Thermodyn.* **1999**, *31*, 1025−1044.

(6) Ortega, J.; Espiau, F.; Toledo, F. J.; Dieppa, R. Thermodynamic Properties of (an Ester+an Alkane). XVII. Experimental H_m^E and V_m^E Values for (an Alkyl Propanoate+ an Alkane) at 318.15 K. *J. Chem. Thermodyn.* **2005**, *37*, 967−983.

(7) Toledo-Marante, F. J.; Ortega, J.; Chaar, M.; Vidal, M. Thermodynamic Properties of (a Butyl Ester+an-Alkane). XIII. H_m^E and V_m^E for {$xCH_3(CH_2)_{u-1}CO_2(CH_2)_3$+(1-$x$) $CH_3(CH_2)_{2v+1}$ CH_3},

where u = 1 to 3 and v = 1 to 7. *J. Chem. Thermodyn.* **2000**, *32*, 1013−1036.

(8) Ortega, J.; Peña, J.; de Alfonso, C. Isobaric Vapor-Liquid Equilibria of Ethyl Acetate+Ethanol Mixtures at 760 ± 0.5 mmHg. *J. Chem. Eng. Data* **1986**, *31*, 339−342.

(9) Ríos, R.; Ortega, J.; Fernández, L.; de Nuez, I.; Wisniak, J. Improvements in the Experimentation and the Representation of Thermodynamic Properties (iso-*p* VLE and *y*^E) of Alkyl Propanoate +Alkane Binaries. *J. Chem. Eng. Data* **2014**, *59*, 125−142.

(10) Ortega, J.; Espiau, F.; Wisniak, J. New parametric model to correlate the excess Gibbs function and thermodynamic properties of multicomponent systems. Application to binary systems. *Ind. Eng. Chem. Res.* **2010**, *49*, 406−421.

(11) Pérez, E.; Ortega, J.; Fernández, L.; Wisniak, J.; Canosa, J. Contributions to the Modeling and Behavior of Solutions Containing Ethanoates and Hydrocarbons. New Experimental Data for Binaries of Butyl Ester with Alkanes (C5-C10). *Fluid Phase Equilib.* **2016**, *412*, 79−93.

(12) Wisniak, J.; Ortega, J.; Fernández, L.; et al. A Fresh Look at the Thermodynamic Consistency of Vapour-Liquid Equilibria Data. *J. Chem. Thermodyn.* **2017**, *105*, 385−395.

(13) Fernández Luís, L.; Ortega, J.; Wisniak, J. A Rigorous Method to Evaluate the Consistency of Experimental Data in Phase Equilibria. Application to VLE and VLLE. *AIChE J.* **2017**, *63*, 5125−5148.

(14) Sosa, A.; Fernández, L.; Ortega, J.; Jiménez, L. The Parametrization Problem in the Modeling of the Thermodynamic Behavior of Solutions. An Approach Based on Information Theory Fundamentals. *Ind. Eng. Chem. Res.* **2019**, *58*, 12876−12893.

(15) Fernández Luís, L.; Ortega; Wisniak, J. Extension of the Validation Method for Vapor-Liquid Equilibrium Data to Systems with non-Volatile Components. *AIChE J.* **2019**, *65*, No. e16628.

(16) Riddick, J. A.; Bunger, W. B.; Sakano, T. K. *Organic Solvents: Physical Properties and Methods of Purification*, 4th ed.; Wiley-Interscience: New York, 1986; Vol. *II*.

(17) TRC. Thermodynamic Tables. *Hydrocarbons & Non-Hydrocarbons*; Thermodynamic Research Center; Texas A&M University System: College Station, TX, 1965, extant 2014.

(18) Fárková, J.; Wichterle, I. Vapour Pressures of Some Ethyl and Propyl Esters of Fatty Acids. *Fluid Phase Equilib.* **1993**, *90*, 143−148.

(19) Muñoz, R.; Monton, J. B.; Burguet, M. C.; de la Torre, J. Vapor-Liquid Equilibria in the Ternary System Isobutyl Alcohol +Isobutyl Acetate+Butyl Propionate and the Binary Systems Isobutyl Alcohol+Butyl Propionate, Isobutyl Acetate+Butyl Propionate at 101.3 KPa. *Fluid Phase Equilib.* **2005**, *238*, 65−71.

(20) Ortega, J.; Espiau, F.; Tojo, J.; Canosa, J.; Rodríguez, A. Isobaric Vapor−Liquid Equilibria and Excess Properties for the Binary Systems of Methyl Esters+Heptane. *J. Chem. Eng. Data* **2003**, *48*, 1183−1190.

(21) Ortega, J.; Galvan, S. Vapor-Liquid Equilibria of Propyl Propanoate with 1-Alkanols at 101.32 KPa of Pressure. *J. Chem. Eng. Data* **1994**, *39*, 907−910.

(22) Ortega, J.; Matos, J. S. Estimation of the Isobaric Expansivities from Several Equations of Molar Refraction for Some Pure Organic Compounds. *Mater. Chem. Phys.* **1986**, *15*, 415−425.

(23) Kell, G. S.; Whalley, E. Reanalysis of the Density of Liquid Water in the Range 0−150 °C and 0−1 Kbar. *J. Chem. Phys.* **1975**, *62*, 3496−3503.

(24) Lagourette, B.; Boned, C.; Saint-Guirons, H.; Xans, P.; Zhou, H. Densimeter Calibration Method versus Temperature and Pressure. *Meas. Sci. Technol.* **1992**, *3*, 699−703.

(25) Rios, R.; Ortega, J.; Sosa, A.; Fernández, L. Strategy for the Management of Thermodynamic Data with Application to Practical Cases of Systems Formed by Esters and Alkanes through Experimental Information, Checking-Modeling, and Simulation. *Ind. Eng. Chem. Res.* **2018**, *57*, 3410−3429.

(26) Mrazek, R. V.; Van Ness, H. C. Heats of Mixing: Alcohol-Aromatic Binary Systems at 25°, 35°, and 45 °C. *AIChE J.* **1961**, *7*, 190−195.

(27) Ríos, R.; Ortega, J.; Fernandez, L. Measurements and Correlations of the Isobaric Vapor-Liquid Equilibria of Binary Mixtures and Excess Properties for Mixtures Containing an Alkyl (Methyl, Ethyl) Butanoate with an Alkane (Heptane, Nonane) at 101.3 kPa. *J. Chem. Eng. Data* **2012**, *57*, 3210−3224.

(28) Lagarias, J. C.; Reeds, J. A.; Wright, M. H.; Wright, P. E. Convergence Properties of the Nelder−Mead Simplex Method in Low Dimensions. *SIAM J. Optim.* **1998**, *9*, 112−147.

(29) Ortega, J.; Espiau, F.; Sabater, G.; Postigo, M. A. Correlation and Prediction of Excess Quantities and Vapor-Liquid Equilibria of Alkyl Esters+Tert-Butyl Alcohol: Experimental Data for Propyl Esters +Tert-Butyl Alcohol. *J. Chem. Eng. Data* **2006**, *51*, 730−742.

(30) Ortega, J.; Espiau, F.; Postigo, M. Vapor-Liquid Equilibria at 101.32 KPa and Excess Properties of Binary Mixtures of Butyl Esters +Tert-Butyl Alcohol. *J. Chem. Eng. Data* **2005**, *50*, 444−454.

(31) Lee, B. I.; Kesler, M. G. A Generalized Thermodynamic Correlation Based on Three-Parameter Corresponding States. *AIChE J.* **1975**, *21*, 510−527.

(32) Spencer, C. F.; Danner, R. P. Improved Equation for Prediction of Saturated Liquid Density. *J. Chem. Eng. Data* **1972**, *17*, 236−241.

(33) Tait, P. G. *Physics and Chemistry of the Voyage of HMS Challenger*, 1888; Vol. *2*, pp 941−951.

(34) Pečar, D.; Doleček, V. Isothermal Compressibilities and Isobaric Expansilities of Pentane, Hexane, Heptane and Their Binary and Ternary Mixtures from Density Measurements. *Fluid Phase Equilib.* **2003**, *211*, 109−127.

(35) Camacho-Camacho, L. E.; Galicia-Luna, L. A. Experimental Densities of Hexane + Benzothiophene Mixtures from (313 to 363) K and up to 20 MPa. *J. Chem. Eng. Data* **2007**, *52*, 2455−2461.

(36) Valencia, J. L.; González-Salgado, D.; Troncoso, J.; Peleteiro, J.; Carballo, E.; Romaní, L. Thermophysical Characterization of Liquids Using Precise Density and Isobaric Heat Capacity Measurements As a Function of Pressure. *J. Chem. Eng. Data* **2009**, *54*, 904−915.

(37) Haghbakhsh, R.; Zolghadr, A.; Raeissi, S.; Ayatollahi, S. Investigation of Volumetric Fluid Properties of (Heptane+Hexadecane) at Reservoir Conditions. *J. Nat. Gas Sci. Eng.* **2015**, *22*, 377−394.

(38) Quevedo-Nolasco, R.; Galicia-Luna, L. A.; Elizalde-Solis, O. Compressed Liquid Densities for the (n-Heptane+n-Decane) and (n-Octane+n-Decane) Systems from T = (313 to 363) K. *J. Chem. Thermodyn.* **2012**, *44*, 133−147.

(39) García-Morales, R.; Elizalde-Solis, O.; Zúñiga-Moreno, A.; Bouchot, C.; Gómez-Ramos, F. I.; Arenas-Quevedo, M. G. Volumetric Properties of 2,5-Dimethylfuran in Mixtures with Octane or Dodecane from 293 K to 393 K and Pressures up to 70 MPa. *Fuel* **2017**, *209*, 299−308.

(40) Pečar, D.; Doleček, V. Temperature and Pressure Dependence of Volumetric Properties for Binary Mixtures of N-Heptane and n-Octane. *Acta Chim. Slov.* **2007**, *54*, 538−544.

(41) Lugo, L.; Comuñas, M. J. P.; López, E. R.; Fernández, J. (P,Vm,T,x) Measurements of Dimethyl Carbonate+octane Binary Mixtures: I. Experimental Results, Isothermal Compressibilities, Isobaric Expansivities and Internal Pressures. *Fluid Phase Equilib.* **2001**, *186*, 235−255.

(42) Moodley, K.; Adam, S.; Naidoo, P.; Naidu, S.; Ramjugernath, D. P−ρ−T Data and Modeling for Propan-1-Ol +n-Octane or n-Nonane or n-Decane from 313.15 K to 363.15 K and 1 MPa to 20 MPa. *J. Chem. Eng. Data* **2018**, *63*, 4136−4156.

(43) Morávková, L.; Wagner, Z.; Linek, J. (P,Vm,T) Measurements of (Cyclohexane + Nonane) at Temperatures from 298.15 K to 328.15 K and at Pressures up to 40 MPa. *J. Chem. Thermodyn.* **2007**, *39*, 1637−1648.

(44) Ihmels, E. C.; Gmehling, J. Densities of Toluene, Carbon Dioxide, Carbonyl Sulfide, and Hydrogen Sulfide over a Wide Temperature and Pressure Range in the Sub- and Supercritical State. *Ind. Eng. Chem. Res.* **2001**, *40*, 4470−4477.

(45) Tsonopoulos, C. An Empirical Correlation of Second Virial Coefficients. *AIChE J.* **1974**, *20*, 263−272.

(46) Laumanns, M.; Thiele, L.; Zitzler, E. An Efficient, Adaptive Parameter Variation Scheme for Metaheuristics Based on the Epsilon-Constraint Method. *Eur. J. Oper. Res.* **2006**, *169*, 932−942.

(47) Akaike, H. In *Information Theory and An Extension of the Maximum Likelihood Principle*, 2nd International Symposium on Information Theory;Petrov, B. N.; Csaki, F., Eds.; 1973; pp 267−281.

(48) Burnham, K. P.; Anderson, D. R. Multimodel Inference: Understanding AIC and BIC in Model Selection. *Sociol. Methods Res.* **2004**, *33*, 261−304.

(49) Scrucca, L. GA : A Package for Genetic Algorithms in R. *J. Stat. Software* **2013**, *53*, 1−37.

(50) Scrucca, L. On Some Extensions to GA Package: Hybrid Optimisation, Parallelisation and Islands Evolutionon Some Extensions to GA Package: Hybrid Optimisation, Parallelisation and Islands Evolution. *R J.* **2017**, *9*, 187.

(51) Aspen Plus of Aspentech. *Aspen Physical Properties System 2004.1. Physical Methods and Models*; Aspen Tecnhnology, Inc.: Cambridge, MA, 2004.

(52) Gmehling, J.; Li, J.; Schiller, M. A Modified UNIFAC Model. 2. Present Parameter Matrix and Results for Different Thermodynamic Properties. *Ind. Eng. Chem. Res.* **1993**, *32*, 178−193.